

Orlistat, a novel potent antitumor agent for ovarian cancer: proteomic analysis of ovarian cancer cells treated with Orlistat

HUI-QIONG HUANG^{1*}, JING TANG^{1*}, SHENG-TAO ZHOU¹, TAO YI¹, HONG-LING PENG¹, GUO-BO SHEN², NA XIE², KAI HUANG², TAO YANG², JIN-HUA WU², CAN-HUA HUANG², YU-QUAN WEI² and XIA ZHAO^{1,2}

¹Gynecological Oncology of Biotherapy Laboratory, Department of Gynecology and Obstetrics, West China Second Hospital, Sichuan University, Chengdu, Sichuan; ²State Key Laboratory of Biotherapy and Cancer Center, West China Hospital, Sichuan University, Chengdu, Sichuan, P.R. China

Received February 9, 2012; Accepted March 19, 2012

DOI: 10.3892/ijo.2012.1465

Abstract. Orlistat is an orally administered anti-obesity drug that has shown significant antitumor activity in a variety of tumor cells. To identify the proteins involved in its antitumor activity, we employed a proteomic approach to reveal protein expression changes in the human ovarian cancer cell line SKOV3, following Orlistat treatment. Protein expression profiles were analyzed by 2-dimensional polyacrylamide gel electrophoresis (2-DE) and protein identification was performed on a MALDI-Q-TOF MS/MS instrument. More than 110 differentially expressed proteins were visualized by 2-DE and Coomassie brilliant blue staining. Furthermore, 71 proteins differentially expressed proteins were positively identified via mass spectrometry (MS)/MS analysis. In particular, PKM1/2, a key enzyme involved in tumorigenesis, was found to be significantly downregulated in SKOV3 cells following treatment with Orlistat. Moreover, PKM1/2 was proved to be downregulated in SKOV3 cells by western blot analysis after treatment with Orlistat. Taken together, using proteomic tools, we identified several differentially expressed proteins that underwent Orlistat-induced apoptosis, particu-

larly PKM2. These changes confirmed our hypothesis that Orlistat is a potential inhibitor of ovarian cancer and can be used as a novel adjuvant antitumor agent.

Introduction

In the 1920s, the Nobel Prize winner Otto Warburg observed a marked increase in glycolysis and enhanced lactate production in tumor cells even when maintained in conditions of high oxygen tension (termed Warburg effect), leading to widespread concerns about the metabolic changes in human types of cancer (1). Either as a consequence or as a cause, alterations of cancer cell-intrinsic metabolism have been considered as essential hallmarks of cancer. Among these metabolic changes, *de novo* fatty acid biosynthesis was found elevated in the majority of human types of cancer, such as prostate (2), colorectal (3), ovarian (4), bladder (5), esophageal (6), gastric (7), lung (8), endometrial (9), breast (10) and soft tissue sarcomas (11). Fatty acid synthase (FASN) is regarded as a key regulator of *de novo* fatty acid synthesis and was widely found upregulated in a wide variety of human malignancies and their pre-neoplastic lesions. Recent studies also reveal that FASN is associated with the stage of cancer and indicate a poor prognosis (12). Thus, FASN could be considered as a reliable predictor of recurrence and disease-free survival along with neo-plastic stage (13). *In vivo* treatment with inhibitors of FASN has been proven to lead to markedly decreased survival in human cancer xenografts (14) and silencing of the FASN gene by siRNA also inhibits cancer cell growth and ultimately induces cancer cell apoptosis (15). Therefore, agents that inhibit FASN and the *de novo* fatty-acid synthesis pathways could be considered as novel antitumor strategies.

Orlistat, an anti-obesity drug approved by the US Food and Drug Administration, which possesses extremely low oral bio-availability (16), exhibits anti-proliferative and anti-tumor properties against prostate and breast cancer cells due to its ability to block the lipogenic activity of FASN (16), by acting on the 2.3-A-resolution crystal structure of the thioesterase domain of FASN (17). Orlistat negatively influences FASN activity and has a significant effect on the antitumor activity by inducing remarkable diversification such as a complete G2-M phase loss, S-phase accumulation and the

Correspondence to: Professor Xia Zhao, Gynecological Oncology of Biotherapy Laboratory, Department of Gynecology and Obstetrics, West China Second Hospital, Sichuan University, No. 20, Section 3 South People's Road, Chengdu, Sichuan 610041, P.R. China
E-mail: xia-zhao@126.com

*Contributed equally

Abbreviations: 2-DE, two-dimensional polyacrylamide gel electrophoresis; MALDI-Q-TOF, matrix-assisted laser desorption ionization quadrupole time-of-flight; MOWSE, molecular weight search; ALODA, aldolase A; LDHA, L-lactate dehydrogenase A chain; KP YM, pyruvate kinase muscle isozyme; MS, mass spectrometry; MTT, 3-(4,5-dimethylthiazol-2-yl)-2,5-diphenyl tetrazolium bromide; PI, propidium iodide; CAPS, calcyphosine; FAS, fatty-acid synthase

Key words: Orlistat, antitumor agent, proteomics, ovarian cancer

emerging sub-G1 (apoptotic) cell increase, and repression of the promoter activity of Her2/neu gene (18).

Ovarian cancer is the most common malignancy of the female reproductive tract and is the leading cause of death from gynecologic types of cancer; it is currently the fifth leading cause of female cancer-related mortality (19). Finding a novel therapeutic approach is essential since the 5-year survival rate of women with ovarian cancer is low, despite the fact that significant progress has been made in the therapy of this disease (20).

2-DE based proteomics has been shown to be a powerful tool in rapidly profiling differentially expressed proteins associated with a number of diseases (21-23). In our study, we aimed to investigate the differential expression in Orlistat-treated SKOV3 cells using a 2DE-MS-based proteomics approach, in order to better understand the molecular mechanisms underlying Orlistat-induced tumor repression. In total, more than 110 differentially expressed proteins were found altered between Orlistat-treated and untreated SKOV3 cells, and subsequently 71 proteins were identified by MS analysis. Furthermore, we showed that PKM2 was significantly down-regulated in Orlistat-treated SKOV3 cells, which confirmed the antitumor properties of Orlistat, indicating that Orlistat can be used as a novel adjuvant antitumor agent for ovarian cancer patients.

Materials and methods

Cell culture and treatment. The human epithelial serous cystadenocarcinoma cell line SKOV3 was obtained from the American Type Culture Collection (ATCC, Rockville, MD). Cells were grown in Dulbecco's-modified Eagle's medium (DMEM, Gibco, USA) containing 10% fetal calf serum (Hyclone, USA), penicillin (10^7 U/l) and streptomycin (10 mg/l) at 37°C in a humidified chamber containing 5% CO₂. Orlistat was dissolved in dimethyl sulphoxide (DMSO). When the cells reached 50-70% confluency, the medium was replaced by a fresh culture medium containing Orlistat. Control cells were cultured in a medium containing an equal amount of DMSO instead of Orlistat. For 2-DE analysis, SKOV3 cells were treated with 20 mM Orlistat for 4 days and the media were changed every day. Cells were washed twice by centrifugation in phosphate buffered saline (PBS) and transferred to sterile plastic tubes for storage at -80°C prior to use.

Cell proliferation assay. Cell growth and viability were assessed using an MTT cell proliferation kit (Roche Applied Science). The cells were seeded on 96-well microplates at 2.0×10^3 /well. At 48, 72 and 96 h, the cells were treated with different concentrations of Orlistat and incubated at 37°C in 5% CO₂. The cells were subsequently incubated with 10 μ l of MTT for 4 h, then the media were removed and 150 μ l DMSO were added. We put the plate in a shaker before reading absorbance at 490-nm using a microplate reader (3550-UV, Bio-Rad, USA), after 20 min of incubation. The procedure was repeated three times with similar results. The following formula was used to calculate the inhibition rate of SKOV3 cell proliferation: (1-experimental group OD value/negative control OD value) x 100%. Media-only treated (untreated) cells were considered as the negative control group.

2-DE and image analysis. Cells (1.3×10^8) were lysed in 1 ml lysis buffer (7 M urea, 2 M thiourea, 4% CHAPS, 100 mM DTT, 0.2% pH 3.0-10.0 ampholyte, Bio-Rad, USA) containing protease inhibitor cocktail 8340 (Sigma, St. Louis, MO, USA). Samples were then kept on ice and sonicated for six cycles of 10 sec, with each cycle consisting of 5 sec sonication, followed by a 10 sec break. After centrifugation at 14,000 rpm for 1 h at 4°C, the supernatant was collected and the protein concentrations determined using the DC Protein Assay Kit (Bio-Rad). Protein samples (3 mg) were applied to an immobilized pH gradient (IPG) strip (17 cm, pH 3.0-10.0 NL, Bio-Rad) using a passive rehydration method. After 12-16 h of rehydration, the strips were transferred to an isoelectric focusing (IEF) cell (Bio-Rad) and focused for a total of 60,000 Vh. The second dimension was performed using 12% equilibration. The gels were stained using CBB R-250 (Merck, Germany) and scanned with a Bio-Rad GS-800 scanner. Triplicate samples were analyzed at each time point of treatment to ensure the reproducibility of analyses. The maps were analyzed by PDQuest software Version 6.1 (Bio-Rad). Each gel spot was normalized as a percentage of the total quantity of all spots in that gel and evaluated in terms of OD. Only those spots that changed consistently and significantly (>2.0-fold) were selected for MS analysis.

In-gel digestion. In-gel digestion of proteins was carried out using MS-grade Trypsin Gold (Promega, Madison, WI, USA), according to the manufacturer's instructions. Briefly, spots were cut out of the gel (1-2 mm diameter) using a razor blade, and destained twice with 100 mM NH₄HCO₃/50% acetonitrile (ACN) at 37°C for 45 min in each treatment. Following dehydration and drying, the gels were pre-incubated in 10-20 μ l trypsin solution for 1 h. Samples were then added in adequate digestion buffer (40 mM NH₄HCO₃/10% ACN) to cover the gels and incubated overnight at 37°C. Tryptic digests were extracted using MiliQ water initially, followed by extraction twice with 50% ACN/5% trifluoroacetic acid (TFA) for 1 h each time. The combined extracts were dried in a vacuum concentrator at room temperature. The samples were then subjected to MS analysis.

MALDI-Q-TOF analysis and protein identification. Mass spectra were acquired using a quadrupole time-of-flight (Q-TOF) mass spectrometer (Micromass, Manchester, UK) with a matrix-assisted laser desorption ionization (MALDI) source (Micromass). Tryptic digests were dissolved in 5 μ l of 70% ACN/0.1% TFA, and then 1 μ l of the digestion was mixed with 1 μ l saturated α -cyano-4-hydroxy-cinnamic acid (CHCA) in 50% ACN/0.5% TFA and spotted onto a 96-well target plate. MS/MS was performed in a data-dependent mode in which the top ten most abundant ions for each MS scan were selected for MS/MS analysis. The MS/MS data were acquired and processed using the MassLynx software (Micromass) and MASCOT was used to search the database. Database searches were carried out using the following parameters: database, Swiss-Prot; taxonomy, *Homo sapiens*; enzyme, trypsin; and allowance of one missed cleavage. Carbamidomethylation was selected as a fixed modification and oxidation of methionine was allowed to be variable. The peptide and fragment mass tolerance were at 1 and 0.2 Da, respectively. The data format

selected was Micromass PKL and the instrument selected was MALDI-Q-TOF. Proteins with probability-based MOWSE scores exceeding their threshold ($P < 0.05$) were considered to be positively identified.

Western blot analysis. Collected cells were lysed in RIPA buffer (50 mM Tris-base, 1.0 mM EDTA, 150 mM NaCl, 0.1% SDS, 1% Triton X-100, 1% sodium deoxycholate, 1 mM PMSF) to extract all the proteins and quantified by the DC protein assay Kit (Bio-Rad). Samples were separated by 12% SDS-PAGE and transferred to polyvinylidene difluoride (PVDF) membranes (Amersham Biosciences). The membranes were blocked overnight with PBS containing 0.1% Tween 20 in 5% skimmed milk at 4°C, and subsequently probed by the primary antibodies: rabbit anti-PKM2 (diluted 1:500, Abcam, UK). Blots were incubated with secondary antibody conjugated to horseradish peroxidase for 2 h at room temperature. Target proteins were detected by enhanced chemiluminescence reagents (Amersham Pharmacia Biotech, Piscataway, USA), and β -actin was used as an internal control.

Statistics. All quantitative data are recorded as the means \pm SD. Comparisons between two groups were performed by Student's t-test. Differences among multiple groups were assessed by one-way ANOVA analysis. Relevance analysis of ordinal data was performed by cross χ^2 test. A statistically significant difference was defined as $p < 0.05$.

Results

Proliferation activity of Orlistat-treated SKOV3 cells. The proliferation activity of Orlistat-treated SKOV3 cells was examined using the MTT assays. MTT results showed that the proliferation activity was suppressed by Orlistat in both a dose- and duration-dependent manner, and the proliferation ratio was decreased to 60% of the control value 96 h after treatment with Orlistat when the drug concentration was 20 mM, as shown in Fig. 1.

Proteomic analysis of Orlistat-treated SKOV3 cell protein expression compared with the parental SKOV3 cells. To explore the molecular mechanisms underlying the Orlistat-induced antitumor activity of SKOV3 cells, 2-DE based proteomics was used to profile differentially expressed proteins in SKOV3 cells treated with or without Orlistat. Image analysis was performed using PDQuest 7.1 software. Representative 2-DE maps are shown in Fig. 2. Approximately 1000-1100 protein spots were detected by CBB R-250 staining in a single 2-DE gel. Each protein spot was normalized as a percentage of the total intensity of all spots in the gel. By comparing 2-DE patterns, differentially expressed proteins were defined as statistically meaningful ($p < 0.05$) based on both of the following two criteria: i) intensity alterations of >2.0 -fold (t-test, $p < 0.05$) and ii) observed in at least 3 individual experiments. According to these criteria, a total of 111 spots were selected and analyzed using MALDI-Q-TOF tandem mass spectrometry. A total of 71 proteins from the 111 spots were identified (Fig. 2). As different isoforms of a protein might have distinct functions, each isoform/spot was considered to be a single protein for analysis in our study.

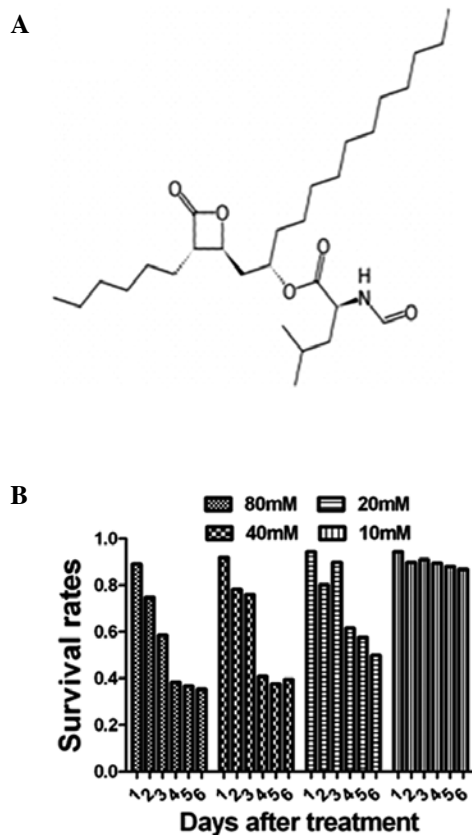


Figure 1. (A) Molecular structure of Orlistat. (B) Inhibitory effect of Orlistat on SKOV3 cell proliferation *in vitro*. Proliferation of the SKOV3 cells was assessed by the MTT assay. Data were assessed as percentage of cell viability in terms of media-only treated (non-treated) control cells at each drug concentration with different times and at each time with a different drug concentration. Orlistat caused a dose- and time-dependent inhibition of proliferation *in vitro*. Means \pm SD (n=3). $P < 0.05$.

Protein identification and bioinformatics analysis. In total, 71 spots with differential expression levels were subjected to MS/MS analysis. The MS/MS data were queried using the search algorithm MASCOT against the ExPASy protein sequence database. Proteins were identified based on a number of criteria including PI, MW, the number of matched-peptides and MOWSE score (Table I and II).

The identified proteins were divided into various groups based on their biological functions and subcellular localization. This implicated roles in metabolism (32%), protein folding (8%), translation (5%), protein modification (4%), cell proliferation (15%), apoptosis (10%), signal transduction (14%) and cell cytoskeleton (12%). The proteins were found to be located in the cytoplasm (57%), nucleus (11%), mitochondrion (15%), cell membrane (10%) or were secreted (12%) (Fig. 2). For a macroscopic presentation, cluster maps and protein interaction and function networks were generated using Cluster or the KEGG-based software tool Cytoscape, respectively. Twenty-three proteins, accounting for 32% of the proteins identified, were found to be associated with metabolism regulation. The metabolism-regulating proteins were grouped in different clusters. Pyruvate kinase isozymes M1/M2 were found to show one of the most significant differences in expression between SKOV3 cells treated with or without

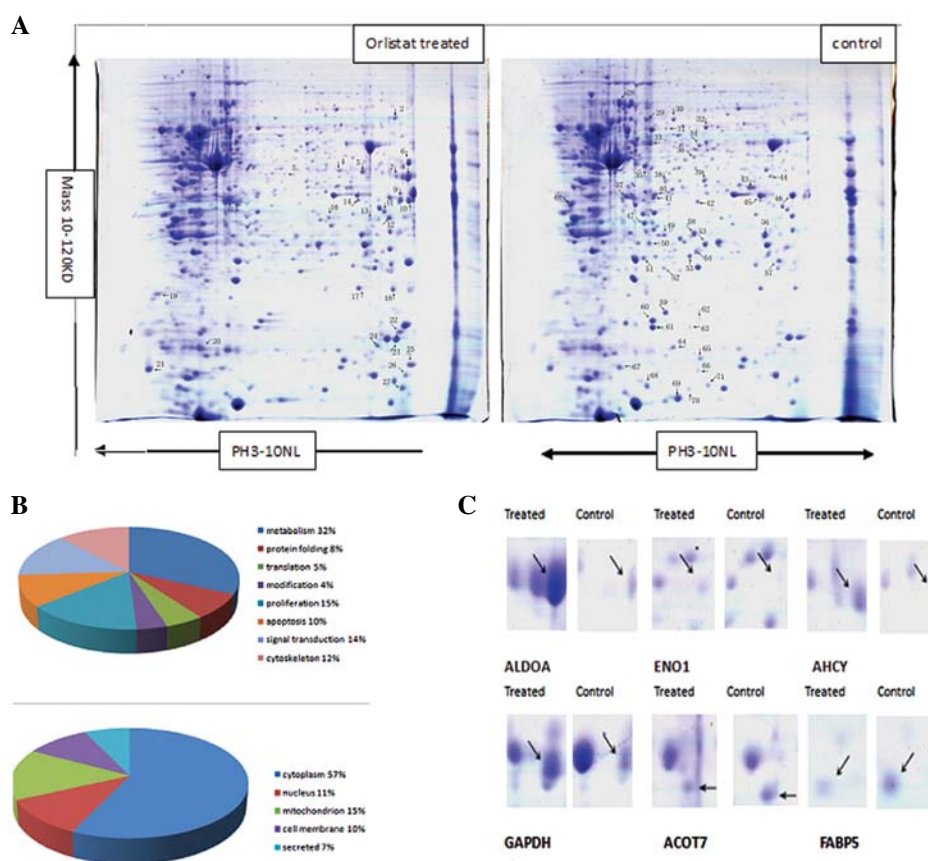


Figure 2. Comparison of the protein expression patterns between control and Orlistat-treated SKOV3 cells. (A) Representative 2-D gel images of the human ovarian cancer cell line SKOV3 treated with or without Orlistat. Total protein extracts were separated on pH 3.0-10.0 nonlinear IPG strips in the first dimension followed by 12% SDS-PAGE in the second dimension and visualized by Coomassie brilliant blue (CBB) staining. Seventy-one differentially expressed spots (27 upregulated and 44 downregulated in Orlistat-treated SKOV3 cells) were identified (as numbered). Details for each numbered spot are reported in Table I. (B) Seventy-one identified proteins were classified into 8 groups. These included metabolism (32%), protein folding (8%), translation (5%), protein modification (4%), cell proliferation (15%), apoptosis (10%), signal transduction (14%) and cell cytoskeleton (12%). These proteins were also found to be located in the cytoplasm (57%), nucleus (11%), mitochondrion (15%), cell membrane (10%) or were secreted (12%). (C) Enlargement of selected regions. Spots selected are ALDOA (Spot 8), ENO1 (Spot 3), AHCY (Spot 7), GAPDH (Spot 9), ACOT7 (Spot 44), FABP5 (Spot 65).

Table I. Protein spots identified by MALDI-Q-TOF.

Spot no.	Accession no. ^b	Protein name ^a	Gene name	Mw ^c	PI ^c	No. of peptide	Coverage (%)	Score ^d
Upregulated								
1	P15311	Ezrin	EZR	69,484	5.94	5	6	133
2	P68104	Elongation factor 1- α 1	EEF1A1	50,451	9.10	15	28	179
3	P06733	α -enolase	ENO1	47,481	7.01	8	18	57
4	P04264	Keratin, type II cytoskeletal 1	KRT1	66,170	8.15	3	3	68
5	P50453	Serpin B9	SERPINB9	43,004	5.61	27	46	372
6	O00429	Dynamin-1-like protein	DNM1L	82,339	6.37	3	4	39
7	P23526	S-adenosyl-L-homocysteine hydrolase	AHCY	48,255	5.92	16	24	86
8	P04075	Fructose-bisphosphate aldolase A	ALDOA	39,851	8.30	56	68	723
9	P04406	Glyceraldehyde-3-phosphate dehydrogenase	GAPDH	36,201	8.57	27	55	400
10	P22626	60S acidic ribosomal protein P0	RPLP0	37,464	8.97	12	41	238
11	P45880	Voltage-dependent anion-selective channel protein 2	VDAC2	32,060	7.49	10	29	91
12	P63244	Guanine nucleotide-binding protein subunit β -2-like 1	GNB2L1	35,511	7.60	12	52	101
13	Q15056	Eukaryotic translation initiation factor 4H	EIF4H	27,425	6.67	7	28	125

Table I. Continued.

Spot no.	Accession no. ^b	Protein name ^a	Gene name	Mw ^c	PI ^c	No. of peptide	Coverage (%)	Score ^d
14	P04083	Annexin A1	Annexin I	38,918	6.57	7	12	45
15	P52907	F-actin-capping protein subunit α -1	CAPZA1	33,073	5.45	8	48	176
16	Q16740	Putative ATP-dependent Clp protease proteolytic subunit, mitochondrial	CLPP	30,446	8.26	2	10	116
17	P07355	Annexin A2	ANXA2	38,808	7.57	45	54	885
18	Q99497	Protein DJ-1	PARK7	20,050	6.33	13	30	97
19	P30048	Thioredoxin-dependent peroxide reductase, mitochondrial	PRDX3	28,017	7.67	9	20	115
20	P04792	Heat shock protein β -1	HSPB1	22,826	5.98	6	37	48
21	P62158	Calmodulin	CALM1	16,827	4.09	6	30	84
22	P60981	Destrin	DSTN	18,950	8.06	8	33	91
23	P00441	Superoxide dismutase	SOD1	16,154	5.70	14	32	140
24	P30044	Peroxiredoxin-5, mitochondrial	PRDX5	22,301	8.93	28	56	281
25	Q04837	Single-stranded DNA-binding protein, mitochondrial	SSBP1	17,249	9.59	8	32	76
26	P07737	Profilin-1	PFN1	15,216	8.44	9	57	135
27	P61088	Ubiquitin-conjugating enzyme E2 N	UBE2N	17,184	6.13	7	36	42
Downregulated								
28	P11142	Heat shock cognate 71 kDa protein	HSPA8	71,082	5.37	50	28	562
29	P35232	Prohibitin	PHB	29,843	5.57	29	51	440
30	P17987	T-complex protein 1 subunit α	TCP1	60,819	5.80	28	37	170
31	P30101	Protein disulfide-isomerase A3	PDIA3	57,146	3.47	7	12	69
32	P78371	T-complex protein 1 subunit β	CCT2	57,794	6.01	36	49	446
33	P14618	Pyruvate kinase isozymes M1/M2	PKM2	58,470	7.96	26	36	309
34	Q9BWD1	Acetyl-CoA acetyltransferase	ACAT2	41,838	6.47	12	41	86
35	P34949	Mannose-6-phosphate isomerase	MPI	47,196	5.62	2	7	38
36	P09972	Fructose-bisphosphate aldolase C	ALDOC	39,830	6.41	13	15	205
37	P68363	Tubulin α -1B	TUBA1B	50,804	4.94	35	41	513
38	P50213	Isocitrate dehydrogenase (NAD) subunit α , mitochondrial	IDH3A	40,022	6.47	22	49	152
39	P37837	Transaldolase	TALDO1	37,688	6.36	23	37	363
40	P07195	L-lactate dehydrogenase B chain	LDHB	36,900	5.71	12	41	86
41	O00764	Pyridoxal kinase	PDXK	35,308	5.75	18	42	175
42	O00487	26S proteasome non-ATPase regulatory subunit 14	PSMD14	34,726	6.06	14	62	62
43	P11177	Pyruvate dehydrogenase E1 component subunit β , mitochondrial	PDHB	39,550	6.20	14	16	186
44	O00154	Cytosolic acyl coenzyme A thioester hydrolase	ACOT7	42,454	8.85	13	25	177
45	P15121	Aldose reductase	AKR1B1	36,230	6.51	40	11	62
46	P00338	L-lactate dehydrogenase A chain	LDHA	36,950	8.44	40	52	319
47	P31937	3-hydroxyisobutyrate dehydrogenase, mitochondrial	HIBADH	35,705	8.38	1	4	39
48	P12004	Proliferating cell nuclear antigen	PCNA	29,092	4.57	45	54	559
49	Q06830	Peroxiredoxin-1	PRDX1	22,324	8.27	2	18	60
50	Q13162	Peroxiredoxin-4	PRDX4	30,749	5.86	3	14	29
51	P00491	Purine nucleoside phosphorylase	PNP	32,325	6.45	4	5	35
52	P30086	Phosphatidylethanolamine-binding protein 1	PEBP1	21,158	7.01	36	62	432

Table I. Continued.

Spot no.	Accession no. ^b	Protein name ^a	Gene name	Mw ^c	PI ^c	No. of peptide	Coverage (%)	Score ^d
53	P60174	Triosephosphate isomerase	TPI1	26,938	6.45	15	57	136
54	P49720	Proteasome subunit β type-3	PSMB3	23,219	6.14	7	30	50
55	Q15185	Prostaglandin E synthase 3	PTGES3	18,971	4.35	6	18	90
56	Q99714	3-hydroxyacyl-CoA dehydrogenase type-2	HSD17B10	27,134	7.66	42	73	632
57	P62826	GTP-binding nuclear protein Ran	RAN	24,579	7.01	4	18	19
58	P42126	Enoyl-CoA δ isomerase 1, mitochondrial	ECI1	33,080	8.80	5	8	60
59	P15531	Nucleoside diphosphate kinase A	NME1	17,309	5.83	19	59	192
60	P62937	Peptidyl-prolyl cis-trans isomerase A	PPIA	18,229	7.68	22	61	327
61	P16949	Stathmin	STMN1	17,292	5.76	18	24	608
62	P24666	Low molecular weight phosphotyrosine protein phosphatase	ACP1	18,487	6.30	4	22	27
63	Q9UHV9	Prefoldin subunit 2	PFDN2	16,695	6.20	1	9	46
64	P62942	Peptidyl-prolyl cis-trans isomerase	FKBP1A	12,000	7.88	3	27	26
65	Q01469	Fatty acid-binding protein, epidermal	FABP5	15,497	6.60	9	37	90
66	O60925	Prefoldin subunit 1	PFDN1	14,202	6.32	2	9	46
67	P35080	Profilin-2	PFN2	15,378	6.55	18	30	179
68	Q99584	Protein S100-A13	S100A13	11,464	5.91	2	22	28
69	P04264	Keratin, type II cytoskeletal 1	KRT1	66,170	8.15	8	11	28
70	P31949	Protein S100-A11	S100A11	11,847	6.56	4	15	36
71	P14174	Macrophage migration inhibitory factor	MIF	12,639	7.74	16	17	366

^aFor several proteins, a few isoforms were identified in the same individual; ^baccession numbers were derived from the ExPASy database; ^ctheoretical molecular mass (kDa) and PI from the ExPASy database; ^dprobability-based MOWSE (molecular weight search) scores.

Table II. Proteins identified to be involved in the metabolic process.

Spot no.	Accession no.	Protein name	Average ratio	Subcellular location	Main function
3	P06733	α -enolas	10.54	Cell membrane	Glycolysis
7	P23526	S-adenosyl-L-homocysteine hydrolase	8.91	Cytoplasm	Control of methylations
8	P04075	Fructose-bisphosphate aldolase A	23.57	Cytoplasm	Glycolysis and gluconeogenesis
9	P04406	Glyceraldehyde-3-phosphate dehydrogenase	4.72	Cytoplasm	Glycolysis
31	P30101	Protein disulfide-isomerase A3	0.23	Cytoplasm	Cysteine-type endopeptidase activity
33	P14618	Pyruvate kinase isozymes M1/M2	0.08	Cytoplasm	Glycolysis
34	Q9BWD1	Acetyl-CoA acetyltransferase	0.22	Cytoplasm	Acetyl-CoA C-acetyltransferase activity
35	P34949	Mannose-6-phosphate isomerase	0.73	Cytoplasm	Mannose-6-phosphate isomerase activity
36	P09972	Fructose-bisphosphate aldolase C	0.19	Cytoplasm	Glycolysis and gluconeogenesis

Table II. Continued.

Spot no.	Accession no.	Protein name	Average ratio	Subcellular location	Main function
38	P50213	Isocitrate dehydrogenase (NAD) subunit α , mitochondrial	0.17	Mitochondrion	Tricarboxylic acid cycle
39	P37837	Transaldolase	0.43	Cytoplasm	Pentose-phosphate pathway
40	P07195	L-lactate dehydrogenase B chain	0.34	Cytoplasm	(S)-lactate + NAD ⁺ = pyruvate + NADH.
43	P11177	Pyruvate dehydrogenase E1 component subunit β , mitochondrial	0.32	Mitochondrion	Pyruvate dehydrogenase (acetyl-transferring) activity
44	O00154	Cytosolic acyl coenzyme A thioester hydrolase	0.37	Mitochondrion	Fatty-acyl-CoA binding
45	P15121	Aldose reductase	0.31	Cytoplasm	Catalytic efficiencies
46	P00338	L-lactate dehydrogenase A chain	0.23	Cytoplasm	L-lactate dehydrogenase activity
47	P31937	3-hydroxyisobutyrate dehydrogenase, mitochondrial	0.33	Mitochondrion	3-hydroxyisobutyrate dehydrogenase activity
51	P00491	Purine nucleoside phosphorylase	0.27	Cytoplasm	Immune response
53	P60174	Triosephosphate isomerase	0.47	Cytoplasm	Triose-phosphate isomerase activity
55	Q15185	Prostaglandin E synthase 3	0.35	Cytoplasm	Molecular chaperone
56	Q99714	3-hydroxyacyl-CoA dehydrogenase type-2	0.41	Mitochondrion	3-hydroxy-2-methylbutyryl-CoA dehydrogenase activity
58	P42126	Enoyl-CoA delta isomerase 1, mitochondrial	0.38	Mitochondrion	Dodecenoyl-CoA delta-isomerase activity
65	Q01469	Fatty acid-binding protein, epidermal	0.27	Cytoplasm	High specificity for fatty acids

Orlistat. It was downregulated more than 10-fold in SKOV3 cells treated with Orlistat compared to those without Orlistat, and MS/MS analysis revealed 15 matched peptides with 36% sequence coverage and a MOWSE score of 309 (Fig. 3).

Proteomic validation of identified proteins. The expression level of PKM2 was further validated by western blotting. Consistent with the observations in 2-DE analysis, PKM2 was downregulated in the Orlistat-treated SKOV3 cells compared with the parental SKOV3 cells. A similar change in the expression level of FASN was detected in SKOV3 cells treated with Orlistat (Fig. 5).

Discussion

Altered expression of lipid metabolic enzymes is a feature of various types of cancer, including those that develop in ovarian tissues (24). Highly proliferating cancer cells need to synthesize fatty acids *de novo* to continually provide lipids for membrane production. The synthesized fatty acids are also used for energy production through β -oxidation and lipid modification of proteins (Fig. 4). FASN, one of the key enzymes involved in *de novo* fatty-acid synthesis, was found to

be overexpressed in various human types of cancer, including prostate, ovary, colon, and lung (25). FASN has been found to be essential for ovarian cancer cell survival and inhibition of FASN activity has been shown to have potential chemopreventive (26) and therapeutic applications (27).

In this study, we found that treatment with Orlistat, an inhibitor of FASN, promoted the apoptosis of SKOV3 cells (Fig. 1). We confirm the inhibitory effect of Orlistat on FASN by western blot analysis using the ovarian cancer cells (SKOV3) as a model, and we found that FASN was 2-fold downregulated after treatment with Orlistat. As shown in Fig. 5, we employed a 2-DE-based proteomics approach to annotate the altered proteins in the SKOV3 cells prior to and following treatment with Orlistat. Our proteomic analysis revealed a total of 71 differentially expressed proteins, which were associated with cell metabolism, proliferation and/or apoptosis.

Among them, Profilin 1, a member of the profilin family, also known as PFN1, was ubiquitous and upregulated more than 10-fold in SKOV3 cells after treatment with Orlistat. PFN1 was found to be involved in multiple cell behaviors, such as cell adhesion, growth, proliferation and signal transduction (34,35). Moreover, 23 proteins were found differentially expressed related to metabolism. Among them,

demonstrated that PKM2 expression is necessary for aerobic glycolysis and cell proliferation *in vivo* (28,30). Knockdown of PKM2 using RNA interference significantly impairs cell growth in tissue culture, inhibition of PKM2 with peptide aptamers inhibits cell proliferation, and PKM2 expression is necessary for both aerobic glycolysis and tumor growth *in vivo* (31,32). It has been proven that the downregulation of PKM2 activity in cancer cells aids in shunting key glycolytic intermediates toward pathways where they, in turn, are utilized as precursors for lipid, amino acid and nucleic acid synthesis. Therefore, the downregulation of PKM2 activity provides a purposeful divergence from catabolic metabolism aimed at energy production toward an anabolic state aimed at providing the needed resources for rapid cellular construction (33). Research has also shown that PKM2 plays a general role in caspase- and Bcl-independent apoptosis, thereby validating PKM2 as a promising, generally relevant target for the development of anticancer therapies with broad efficacy (34). In our study, PKM was downregulated more than 10-fold, confirming our hypothesis that Orlistat has antitumor abilities. Furthermore, significant downregulation of PKM2 after treatment with Orlistat was confirmed in the ovarian cancer cell line SKOV3 cells by western blot analysis.

In conclusion, using proteomic tools, we identified 71 differentially expressed proteins following Orlistat treatment of ovarian cancer cells. The functions of the differentially expressed proteins were correlated to apoptosis and/or anti-proliferation cellular processes. These results support the hypothesis that Orlistat is a potential inhibitor of ovarian cancer and can be used as a novel assistant antitumor agent, combined with conventional surgical resection and chemotherapy.

Acknowledgements

This work was supported by the National Key Basic Research Program (973 Program) of China (2011CB910703).

References

- Clemens MJ: Targets and mechanisms for the regulation of translation in malignant transformation. *Oncogene* 23: 3180-3188, 2004.
- Bull JH, Ellison G and Patel A, *et al*: Identification of potential diagnostic markers of prostate cancer and prostatic intraepithelial neoplasia using cDNA microarray. *Br J Cancer* 84: 1512-1519, 2001.
- Rashid A, Pizer ES, Moga M, *et al*: Elevated expression of fatty acid synthase and fatty acid synthetic activity in colorectal neoplasia. *Am J Pathol* 150: 201-208, 1997.
- Gansler TS, Hardman W III, Hunt DA, *et al*: Increased expression of fatty acid synthase (OA-159) in ovarian neoplasms predicts shorter survival. *Hum Pathol* 18: 686-692, 1997.
- Gansler TS, Hardman W III, Hunt DA, *et al*: Immunohistochemical expression and prognostic significance of FAS and GLUT1 in bladder carcinoma. *Anticancer Res* 23: 335-339, 2003.
- Nemoto T, Terashima S, Kogure M, *et al*: Overexpression of fatty acid synthase in oesophageal squamous cell dysplasia and carcinoma. *Pathobiology* 69: 297-303, 2001.
- Kusakabe T, Nashimoto A, Honma K and Suzuki T: Fatty acid synthase is highly expressed in carcinoma, adenoma and in regenerative epithelium and intestinal metaplasia of the stomach. *Histopathology* 40: 71-79, 2002.
- Piyathilake CJ, Frost AR, Manne U, *et al*: The expression of fatty acid synthase (FAS) is an early event in the development and progression of squamous cell carcinoma of the lung. *Hum Pathol* 31: 1068-1073, 2000.
- Pizer ES, Lax SF, Kuhajda FP, Pasternack GR and Kurman RJ: Fatty acid synthase expression in endometrial carcinoma: correlation with cell proliferation and hormone receptors. *Cancer* 83: 528-537, 1998.
- Alò PL, Visca P, Marci A, Mangoni A, Botti C and Di Tondo U: Expression of fatty acid synthase (FAS) as a predictor of recurrence in stage I breast carcinoma patients. *Cancer* 77: 474-482, 1996.
- Pizer ES, Wood FD, Heine HS, Romantsev FE, Pasternack GR and Kuhajda FP: Inhibition of fatty acid synthase delays disease progression in a xenograft model of ovarian cancer. *Cancer Res* 56: 189-193, 1996.
- Alò PL, Visca P, Botti C, *et al*: Immunohistochemical expression of human erythrocyte glucose transporter and fatty acid synthase in infiltrating breast carcinomas and adjacent typical/atypical hyperplastic or normal breast tissue. *Am J Clin Pathol* 116: 129-134, 2001.
- Alò PL, Visca P, Framarino ML, *et al*: Immunohistochemical study of fatty acid synthase in ovarian neoplasms. *Oncol Rep* 7: 1383-1388, 2000.
- Costello LC and Franklin RB: 'Why do tumour cells glycolyse?': from glycolysis through citrate to lipogenesis. *Mol Cell Biochem* 280: 1-8, 2005.
- De Schrijver E, Brusselmans K, Heyns W, Verhoeven G and Swinnen JV: RNA interference-mediated silencing of the fatty acid synthase gene attenuates growth and induces morphological changes and apoptosis of LNCaP prostate cancer cells. *Cancer Res* 63: 3799-3804, 2003.
- Menendez JA, Vellon L and Lupu R: Orlistat: From antiobesity drug to anticancer agent in Her-2/neu (erbB-2)-overexpressing gastrointestinal tumors? *Exp Biol Med* (Maywood) 230: 151-154, 2005.
- Pemble CW IV, Johnson LC, Kridel SJ and Lowther WT: Crystal structure of the thioesterase domain of human fatty acid synthase inhibited by Orlistat. *Nat Struct Mol Biol* 14: 704-709, 2007.
- Knowles LM, Axelrod F, Browne CD and Smith JW: A fatty acid synthase blockade induces tumor cell-cycle arrest by down-regulating Skp2. *J Biol Chem* 279: 30540-30545, 2004.
- Jemal A, Siegel R, Ward E, Hao Y, Xu J, Murray T and Thun MJ: Cancer statistics. *CA Cancer J Clin* 58: 71-96, 2008.
- Raki M, Rein DT, Kanerva A and Hemminki A: Gene transfer approaches for gynecological diseases. *Mol Ther* 14: 154-163, 2006.
- Liu R, Li Z, Bai S, *et al*: Mechanism of cancer cell adaptation to metabolic stress: proteomics identification of a novel thyroid hormone-mediated gastric carcinogenic signaling pathway. *Mol Cell Proteomics* 8: 70-85, 2009.
- Tong A, Wu L, Lin Q, *et al*: Proteomics analysis of cellular protein alterations using a hepatitis B virus-producing cellular model. *Proteomics* 8: 2012-2023, 2008.
- Liu R, Wang K, Yuan K, *et al*: Integrative oncoproteomics strategies for anticancer drug discovery. *Expert Rev Proteomics* 7: 411-429, 2009.
- Medes G, Thomas A and Weinhouse S: Metabolism of neoplastic tissue. IV: A study of lipid synthesis in neoplastic tissue slices *in vitro*. *Cancer Res* 13: 27-29, 1953.
- Witkowski A, Joshi AK and Smith S: Coupling of the de novo fatty acid biosynthesis and lipoylation pathways in mammalian mitochondria. *J Biol Chem* 282: 14178-14185, 2007.
- Chirala SS and Wakil SJ: Structure and function of animal fatty acid synthase. *Lipids* 39: 1045-1053, 2004.
- Kuhajda FP, Jenner K, Wood FD, Hennigar RA, Jacobs LB, Dick JD and Pasternack GR: Fatty acid synthesis: a potential selective target for antineoplastic therapy. *Proc Natl Acad Sci USA* 91: 6379-6383, 1994.
- Christofk HR, Vander Heiden MG, Harris MH, *et al*: The M2 splice isoform of pyruvate kinase is important for cancer metabolism and tumour growth. *Nature* 452: 230-233, 2008.
- Guminska M, Ignacak J, Kedryna T and Stachurska MB: Tumor-specific pyruvate kinase isoenzyme M2 involved in biochemical strategy of energy generation in neoplastic cells. *Acta Biochim Pol* 44: 711-724, 1997.
- Mazurek S, Boschek CB, Hugo F and Eigenbrodt E: Pyruvate kinase type M2 and its role in tumor growth and spreading. *Semin Cancer Biol* 15: 300-308, 2005.
- Dombrackas JD, Santarsiero BD and Mesecar AD: Structural basis for tumor pyruvate kinase M2 allosteric regulation and catalysis. *Biochemistry* 44: 9417-9429, 2005.

32. Spoden GA, Mazurek S, Morandell D, *et al*: Isotype-specific inhibitors of the glycolytic key regulator pyruvate kinase subtype M2 moderately decelerate tumor cell proliferation. *Int J Cancer* 123: 312-321, 2008.
33. Steták A, Veress R, Ovádi J, Csermely P, Kéri G and Ullrich A: Nuclear translocation of the tumor marker pyruvate kinase M2 induces programmed cell death. *Cancer Res* 67: 1602-1608, 2007.
34. Janke J, Schlüter K, Jandrig B, *et al*: Suppression of tumorigenicity in breast cancer cells by the microfilament protein profilin 1. *J Exp Med* 191: 1675-1686, 2000.
35. Wu N, Zhang W, Yang Y, *et al*: Profilin 1 obtained by proteomic analysis in all-trans retinoic acid-treated hepatocarcinoma cell lines is involved in inhibition of cell proliferation and migration. *Proteomics* 6: 6095-6106, 2006.